CRATER MORPHOMETRY ON VENUS.

C. G. Cochrane, Imperial College, London (c.cochrane@ic.ac.uk).

Introduction: Most impact craters on Venus are pristine, and provide probably the best available analogs for craters on Earth soon after impact; hence the value of measuring their 3-D shape to known accuracy. The USGS list 967 craters: from the largest, Mead at 270 km diameter, to the smallest, unnamed at 1.3 km. Initially, research focussed on the larger craters. Schaber *et al* [1] (11 craters >50 km) and Ivanov *et al* [2] (31 craters >70 km) took crater depth from Magellan altimetry. Sharpton [3] (94 craters >18 km) used floor-offsets in Synthetic Aperture Radar (SAR) F-MIDR pairs, as did Herrick & Phillips [4]. They list many parameters but not depth for 891 craters. The LPI database[1] now numbers 941. Herrick & Sharpton [5] made Digital Elevation Models (DEMs) of all craters at least partially imaged twice down to 12 km, and 20 smaller craters down to 3.6 km. Using FMAP images and the Magellan Stereo Toolkit (MST) v.1, they automated matches every 900m but then manually edited the resultant data.

Sample Selection: This research is of a region astride western Aphrodite Terra, defined in Fig 1, because it has the most contiguous Cycle 3 coverage, plus right-looking coverage (shown in orange) which will be used to validate the DEMs. This sample area is 7.5% of the surface area of the planet and contains 78 craters (8.3%) on the LPI database. Several analyses show that the sample area has typical terrains and representative crater types for Venus. It includes the largest crater, Mead, and youngest, Adivar. Only 57 of the craters are sufficiently well covered in both Cycles 1 & 2 for DEM generation. MST v.2 was used to automatically match down to 2x4 groups of 75m pixels, the smallest group that, at these latitudes, is larger than the largest SAR resolution cell (ie in Cycle 3).

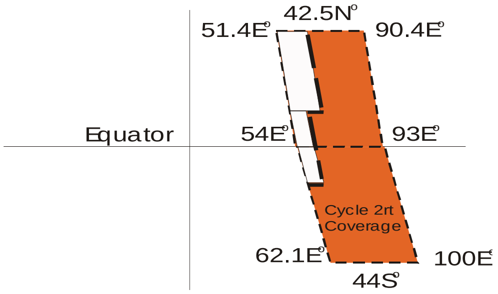

Fig 1 – Sample Area definition

Artifacts: About half the DEMs showed evidence of 3 types of artifact, as reported in [6]:

Matching runaway – a half-cone pointing west obscuring the topography produced by a matching failure propagating east and north/south. Can be minimised if framelets have good texture on the left-hand side.

Prominence extension – features extend down range into a ridge, eg central peak linked to the rim. Probably due to radar shadowing differences, these are easily recognised and avoided during analysis.

Araration (from Latin: *Arare* to plough) consists of parallel furrows some 50 pixels apart, oriented north-south, and at least tens of metres deep. Fig 2, a 75x75 km DEM with times-10 vertical exaggeration and the bright ejecta field of Teumere to lower right, shows araration throughout. It is due to the data compression algorithm threashold and interleaving of resolution cells placing an image transition at a different altitude depending on the combination of the two threshold conditions: either the pink areas in Fig 3 trip the threshold for that cell or the next. Note that the resolution cells in Cycles 1 and 3 are of different size (eg, at Teumere: 186 and 345 m respectively) and in a random phase relationship. Fig 4 shows that the pattern (I, in blue) of altitude errors, for transitions that just trip the threashold, is similar to the furrows in the Teumere DEM. This is the most likely pattern because the compression coding continually adjusts the threashold – see Kwok and Johnson [7]. Fig 4 also shows patterns for brighter transitions: 2I and 4I. The

Fig 2 - Visualisation around Teumere (38S, 88E)

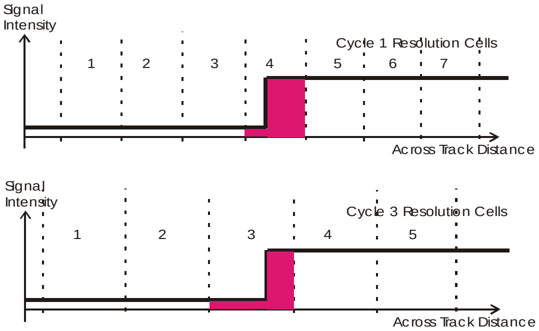

Fig 3 – Timing (Range) Diagram

similarity and periodic nature of these three functions suggest DEMs might be improved by filtering. If not, the most likely (blue) pattern has an inherent root mean square (rms) height error of 77.5m, ie similar to that given by Leberl [8] as "error type 2". There is an additional, lateral error due to resampling at 75m pitch, usually taken as half a pixel (37.5m). In the worst case, these 2 errors sum to 115m.

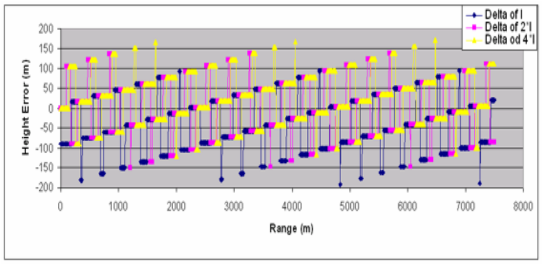

Fig 4 – Typical Error functions at Teumere

DEM Evaluation:

Crater Rims. As reported in [5], diameters given in earlier research have been systematically underestimated, probably because scarps are radar-bright and rounded uplifts pooly delineated. As Fig 5 shows, the average correction is +10% for craters less than 70km.

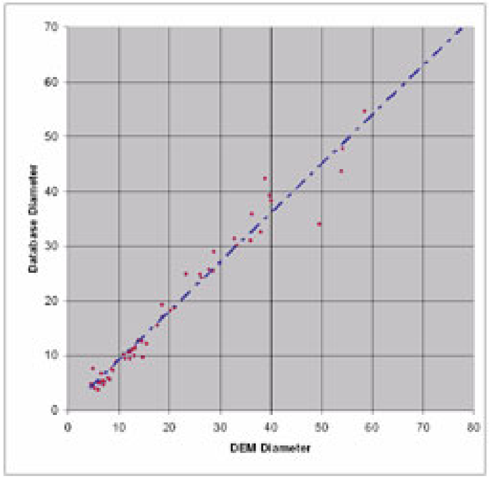

Fig 5 DEM vs Database Diameters.

Depth-Diameter. Fig 6 shows that rim-floor depths and rim diameters (in red) of the 56 DEMs of depth >100m fall close to the trend lines in [2], [3] and [5]. A single trend line is unusually steep; separate trends for small (red triangles) and large (yellow triangles), with a transition at 13km, are more satisfactory: for the larger craters, similar to those for the terrestrial planets given in [2] & [3] and, for smaller craters, parallel to the theoretical slope but offset from it by a factor of about 4. The red dotted lines show the significance of a 115m error. The results for small craters are significantly different to Herrick and Sharpton [5] but rest on an unedited, and 18-fold denser, set of pick points. This trend may indicate that most small craters were formed by "compound" impacts of rubble, with crater diameter due to impactor break-up altitude as shown by Melosh [9] and MacKinnon *et al* [10].

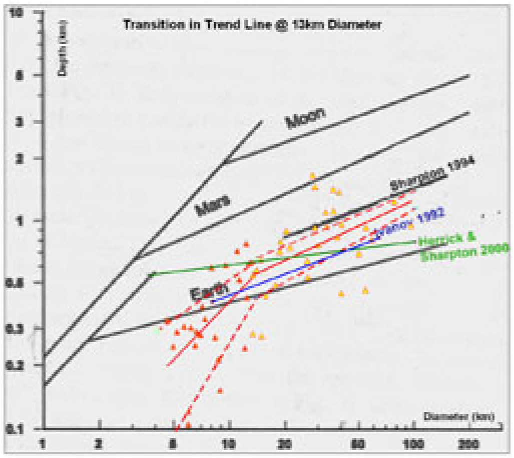

Fig 6 – Depth-Diameter for the Sample

DEM Validation. The Sample includes 17 DEMs (2% of the planetary crater population) with no significant artifacts and a Cycle 2 image for DEM validation. They will be used to validate DEM generation processes, and hence all non-polar MST topography.

Crater Shape. Earlier research gives a host of parameters but none for crater shape to inform 2 key issues: impact angle and post-impact modification. Hence, a genetic algorithm has been designed to match each DEM to an idealised crater geometry.

Conclusion: MST version 2 is proving a useful research tool, providing morphometry of a representative sample of Venusian craters. Its use in investigation of other aspects of the topography of Venus, especially around Aphrodite Terra, is recommended.

References: [1] Schaber, GG *et al* (1992) *JGR 97*, 13257-13302. [2] Ivanov, BA *et al* (1992) *JGR 97* 16167-16181. [3] Sharpton, VI (1994) *GSA SP-293*, 19-27. [4] Herrick, RR & Phillips RJ, (1994) *Icarus 111*, 387-416. [5] Herrick & Sharpton (2000) *JGR 105*, 20245-20262. [6] Cochrane, CG, *Vernadsky-Brown Micro-36* (2002), [7] Kwok, R and Johnson, WTK (1989) *IEEE Transactions on Geoscience & Remote Sensing Vol 27 No 4*, 375-383. [8] Leberl, WF *et al*, (1992) *JGR 97*, 13675-13689. [9] Melosh, H J, *Impact Cratering*, 1989, Oxford Univ Press. [10] McKinnon, W B *et al*. (1997) *Venus II*, 969-1014.

---

[1] See http://www.lpi.usra.edu/research/vc/vchome.html